Malaysian Journal of Chemistry, 2024, Vol. 26(3), 141-150
(Special Issue: *The International Conference on Advanced Materials & Sustainable Energy Technologies 2023*)

Reduced Graphene Oxide Enhances the Performance of $ZnOFe_2O_3$ for Glucose Electrochemical Oxidation

Nur Afifah Mat Razali[1], Norilhamiah Yahya[1]* and Nurul Atiqah Izzati Md Ishak[2]
[1]Section Environmental Engineering Technology, Universiti Kuala Lumpur Malaysian Institute of Chemical and Bioengineering Technology, Lot 1988, Bandar Vendor, 78000 Alor Gajah, Malacca
[2]Research Centre for Nanomaterials and Energy Technology (RCNMET), School of Engineering and Technology, Sunway University, Bandar Sunway, Petaling Jaya, 47500, Selangor Darul Ehsan, Malaysia
*Corresponding author (e-mail: norilhamiah@unikl.edu.my)

The need for accurate analytical glucose measurement techniques that are low-cost, highly sensitive, and user-friendly is crucial for glucose monitoring in healthcare and optimizing industrial processes. A simple and low-cost glucose monitoring was designed by synthesizing Zinc Oxide (ZnO) with Iron Oxide (Fe_2O_3) through a hydrothermal method by loading the composite onto reduced Graphene Oxide. The ZnO nanoparticles had a flower-like shape, while Fe_2O_3 had a sphere-like shape. These nanoparticles were evenly distributed on the wrinkled sheet surface of rGO with an average size of particles of $\pm$ 14.88 nm as observed via Transmission Electron Microscopy (TEM) and Field Emission Scanning Electron Microscopy (FESEM). The X-ray Diffraction (XRD) analysis exhibits overlapping peaks of diffraction of Fe_2O_3 and rGO at 24°, resulting from the reduction of GO. Cyclic Voltammetric analysis (CV) was used to determine the prepared composite's electrochemical properties, which was then further manufactured as a sensing probe. CV analysis revealed that the modified electrode's current response was higher than the bare electrode (ZnO and Fe_2O_3) with and without glucose. The modified glucose sensor shows a sensitivity of 504.23 µA mM^{-1} cm^{-2} and a limit detection of glucose of 6.28 mM.

Keywords: Electrochemical; reduced graphene oxide; metal oxide; glucose oxidation; $ZnOFe_2O_3$

Received: February 2024; Accepted: February 2024

The abnormal glucose level in the body can lead to diabetes, which poses risks to the kidneys, nervous system, and retina [1]. According to data from the World Health Organization (WHO), it was discovered that almost 463 million of the population worldwide had diabetes in 2019, with 90% of them diagnosed with Type 2 diabetes [2]. While the number is expected to increase to 700 million by 2045, this has been a concern not only for medical fields but also the food and beverage companies, which must reduce the sugar level in their products while maintaining the shelf life and quality of the products [2-3]. Due to that, the adoption of non-invasive and quick glucose level monitoring with good stability, high sensitivity and selectivity, as well as inexpensive, is needed for diabetic patients to monitor their blood glucose accurately as well as throughout the manufacturing and final food and beverages production [3]. Past studies have utilized electrochemical sensors for glucose detection, with favorable outcomes including minimal detection limit, an extensive direct response range, good stability performance and selective and sensitive glucose detection. The application of nanoparticles and noble metal oxides in the biosensor is one of the modifications that improve the accuracy and sensitivity of the sensor while enhancing its thermal and electrical properties [4].

Among these metal oxides, Zinc Oxide (ZnO) and Iron Oxide (Fe_2O_3) are potential candidates for improved modification due to high chemical stability, cost-saving and ample availability, non-toxicity and electrochemical properties [1, 5, 6]. Additionally, ZnO and Fe_2O_3 are environmentally friendly, stable semiconductors with good thermal conductivity, chemical stability and high surface activity. [1]. These materials are essential multifunctional semiconductor materials applications ranging from solar cells, transparent conductors, and gas sensors to electrochemical devices [5, 7]. Combining ZnO and Fe_2O_3 induces synergistic effects and enhances electrochemical sensoring activity. Therefore, this combination is expected to have enhanced electrochemical and catalytic properties compared to individual constituent components. Despite this combination's advantages, the electrical conductivity of the $ZnOFe_2O_3$ is still unsatisfactory [1, 8].

This issue can be resolved by incorporating the nanocomposite on a support or substrate with a wide surface area and good stability, which can prevent the aggregation between the $ZnOFe_2O_3$ composite. Graphene with sp^2 is suggested as the ideal electrocatalyst support for its superior electron conductivity, good mechanical and thermal strength and wide

†Paper presented at the International Conference on Advanced Materials & Sustainable Energy Technologies 2023

surface area [1]. Graphene's implementation in the nanotechnology field focuses on further developing semiconductor materials to enhance electrode stability, sensitivity, and selectivity. Reduced Graphene Oxide (rGO), a carbon-sourced nanosheet, can provide an excellent active site and wide surface area for the reagents' adsorption and reaction [6, 9]. The exceptional characteristics of graphene make them a reliable component in preparing metal oxide composite to boost the electrochemical performance of the modified electrodes [10]. Therefore, incorporating rGO and metal oxide nanomaterials is viable as electrode materials for modifying biosensors.

In this research, ZnO will be doped with Fe_2O_3 through hydrothermal loading of $ZnOFe_2O_3$ onto rGO. Characterization tests will examine the surface and structural morphology of the prepared $ZnOFe_2O_3$/rGO composite. At the same time, cyclic voltammetry will be utilized to measure the electrochemical performance of the $ZnOFe_2O_3$/rGO electrode in glucose ranging from 1-10 mM and a scan rate of 10 – 150 mV s^{-1}.

EXPERIMENTAL

Chemicals and Materials

The following chemicals were acquired from Sigma Aldrich: Zinc Nitrate, ($Zn(NO_3)_2 \cdot 6H_2O$), Iron (III) Chloride ($FeCl_3 \cdot 6H_2O$), Graphene Oxide (GO), ethanol, D-glucose ($C_6H_{12}O_6$), and sodium hydroxide pellet. The materials were used without any additional processing or refinement.

Synthesis of $ZnOFe_2O_3$/rGO

$ZnOFe_2O_3$/rGO was prepared hydrothermally, and 50 mg of GO was added to ethanol (5 mL) under a drastic stirring for 15 min. Next, a solution containing 0.1M $Zn(NO_3)_2.6H_2O$) and $FeCl_3.6H_2O$ was introduced into the aforementioned solution while stirring continuously for 30 min. Consequently, aA 10 mL aliquot of NaOH aqueous solution was added to the corresponding solution and ultra-sonicated until the solution achieved homogeneity. The solution was put into a 50 mL Teflon reactor and subjected to heating at 150 ℃ for 7 h. The solution was further filtered using a vacuum pump to isolate solid products and washed with 1 L of deionized water a few times. Finally, the filtered solid product was dried for 7 h at 105 ℃ to get the uniform $ZnOFe_2O_3$ nano-particles embedded in GO. In control studies, ZnO/rGO was synthesized under identical conditions without the inclusion of $FeCl_3 \cdot 6H_2O$ in the first step, and Fe_2O_3/ rGO was synthesized by the same approach without incorporating $Zn(NO_3)_2 \cdot 6H_2O$. Similarly, for ZnO and Fe_2O_3, the synthesis was carried out using the same procedure without including GO. The method of synthesizing the $ZnOFe_2O_3$/rGO composite is depicted in Figure 1.

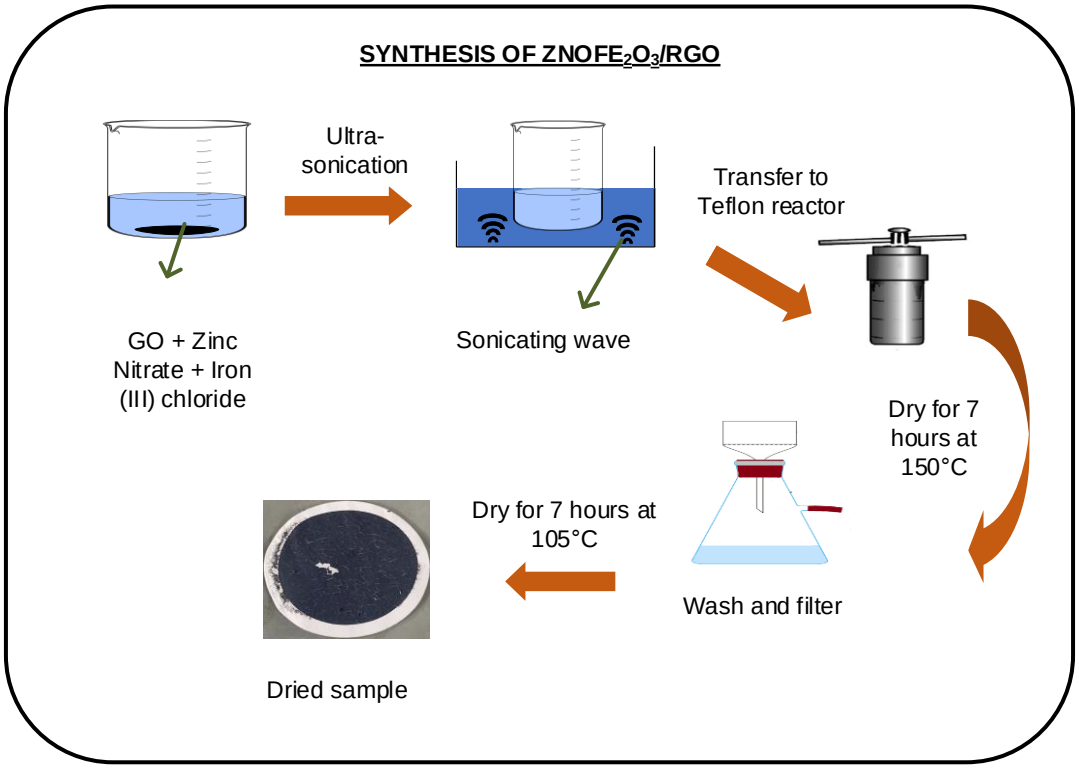

Figure 1. Schematic representation of the nanocomposite synthesis.

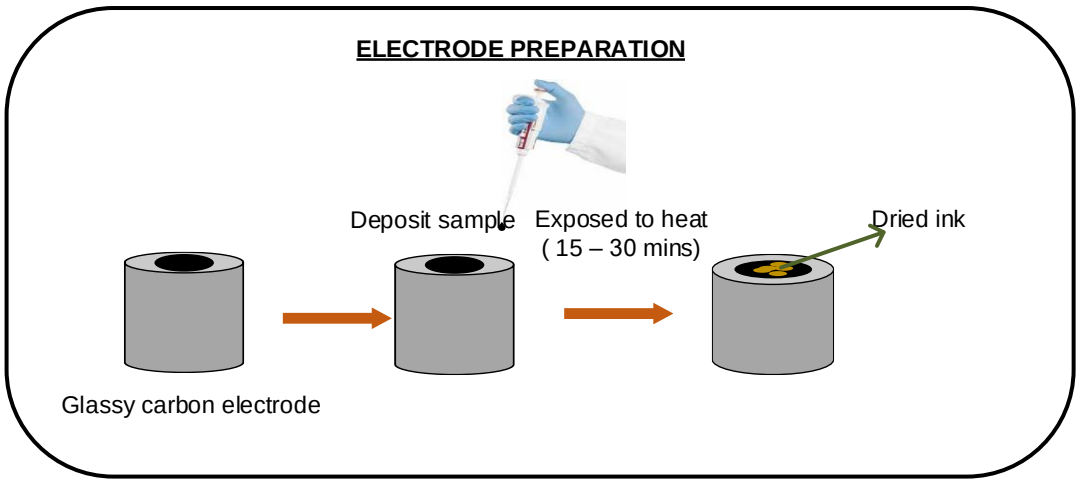

Figure 2. Procedure for the electrode preparation.

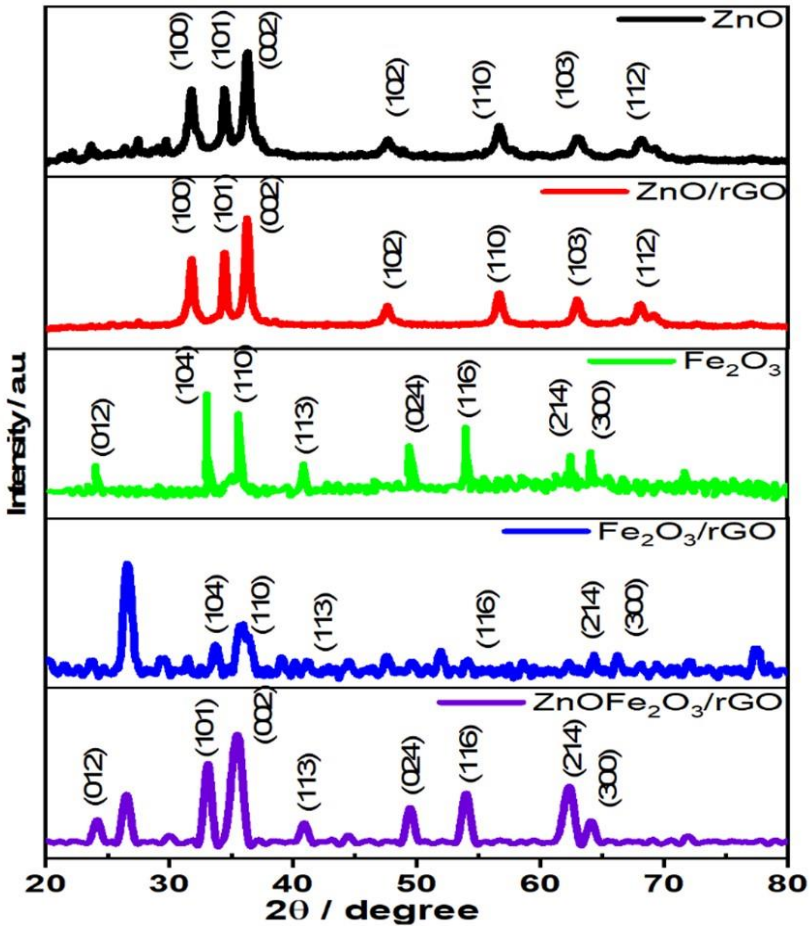

Figure 3. XRD spectrum of ZnO, ZnO/rGO, Fe_2O_3, Fe_2O_3/rGO and $ZnOFe_2O_3$/rGO.

Electrochemical Measurement

The modified electrodes were analyzed through electrochemical using Autolab PGSTAT 204 electrochemical workstation in a three-electrode system. The working electrode used was a Glassy Carbon Electrode (GCE) with a diameter of 3 mm. Ag/AgCl saturated KCl acts as the reference electrode and Pt rod as the counter electrode. 5 µL of the combination of ink catalysts was prepared, containing 150 µL deionized water, 150 µL IPA, 50 µL 5 wt% Nafion and 3.0 mg $ZnOFe_2O_3$/rGO. This mixture was drop cast onto the surface of

GCE and exposed to heat for 15 – 30 min. Correspondingly, Cyclic Voltammogram (CV) tests were run in 0.1 M PBS electrolyte with the presence and absence of 5 mM glucose with scan rates varied at 10, 25, 50, 80, 100, 120, and 150 mV s^{-1} and a sweep potential between -1.0 to 1.0 V.

Physicochemical Characterization

The crystallinity of the composite was investigated using powder X-ray Diffraction (XRD) patterns of the catalysts measured on a PANalytical X'Pert PRO MRD X-ray with Cu Kα as the radiation source (λ = 1.54056 Å) at a scanning rate of 1° in the range of 20°–80°. The structures of $ZnOFe_2O_3$/rGO were examined using Transmission Electron Microscopy (TEM, JEM-200CX) and Field Emission Scanning Electron Microscopy (FESEM, Carl Zeiss).

RESULTS AND DISCUSSION

Physicochemical Characterization

The synthesized $ZnOFe_2O_3$/rGO morphology was first examined by XRD analysis, shown in Figure 3. The XRD pattern for polycrystalline ZnO was the strongest at the (101) plane, while the XRD pattern obtained for ZnO/rGO was similar to ZnO with seven peaks at 31.7°, 34.2°, 36.3°, 47.6°, 62.8° 67.8°corresponds to the (100), (002),(101), (102), (110), (103) and (112) respectively. The obtained peaks follow the JCPDS card #792205. Fe_2O_3 and Fe_2O_3/ rGO exhibit diffraction peaks that are consistent with standard card JCPDS No: 33-0664. Sharp diffraction peaks were obtained, suggesting the high crystallinity of the particles, even after being composited with GO. Figure 3 illustrates the reflection from ZnO and Fe_2O_3 nanoparticles that make up the XRD peaks of $ZnOFe_2O_3$/rGO. The reduction in intensities of ZnO peaks was noticeable compared to Fe_2O_3 peaks, potentially due to the aggregation of Fe_2O_3 particles surrounded by ZnO particles during the synthesis process [11]. Moreover, the reduction of GO during the hydro-thermal process causes overlapping of the subsequent diffraction peaks of Fe_2O_3 and rGO, leading to an increase in the relative intensity peak at 24° [11]. FESEM further confirmed that ZnO remained around the outer layer of the agglomerative hematite while ZnO and Fe_2O_3 bind to the rGO sheets. Additionally, the XRD diffractogram of the composite demonstrates faint reflection peak features of the ZnO wurtzite single phase, which is attributed to the moderately small quantity of ZnO sheet present in the mixture [11-12].

The morphology of ZnO, Fe_2O_3, ZnO/rGO, Fe_2O_3/rGO, and ZnO Fe_2O_3/rGO was measured by FESEM. From Figure 4a, ZnO particles comprise uniform hexagonal nanorod-shaped flower-like nano-particles. Nanosheets with a uniform thickness appeared to stand on each ZnO nanorod, with an estimated particle size of 70 nm. Most of the nano-sheets' planes were perpendicular to the direction of the length of nanorods and parallel to one another, with about an approximately equal distance between them.

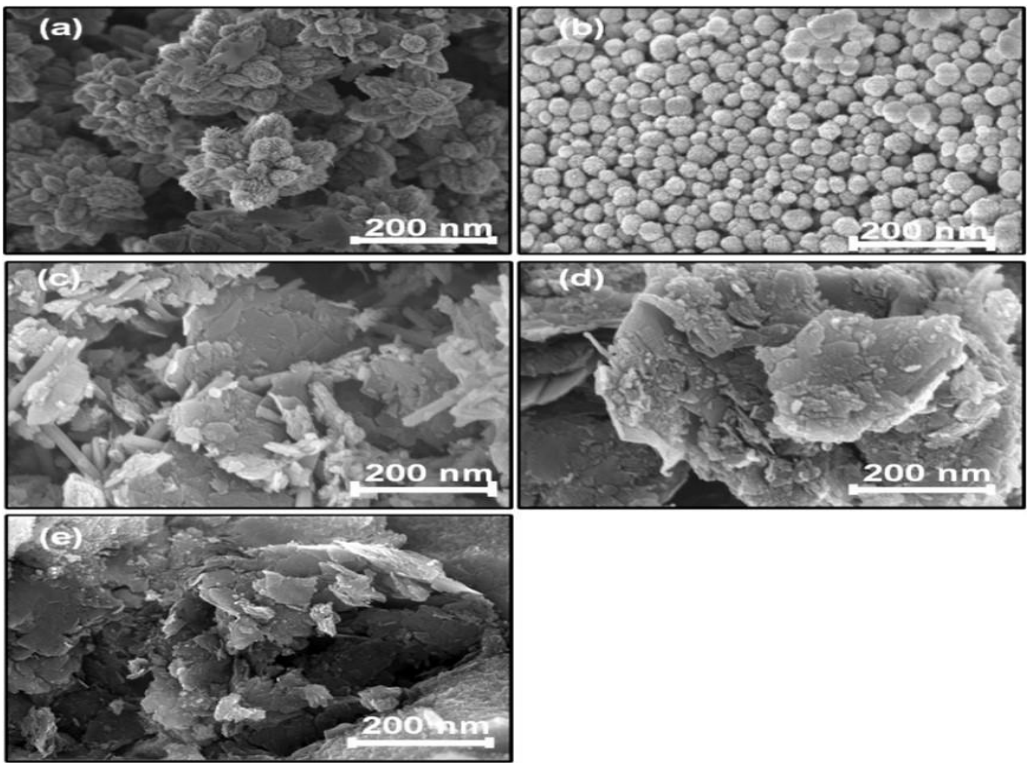

Figure 4. FESEM image of ZnO, Fe_2O_3, ZnO/rGO Fe_2O_3/rGO and $ZnOFe_2O_3$/rGO.

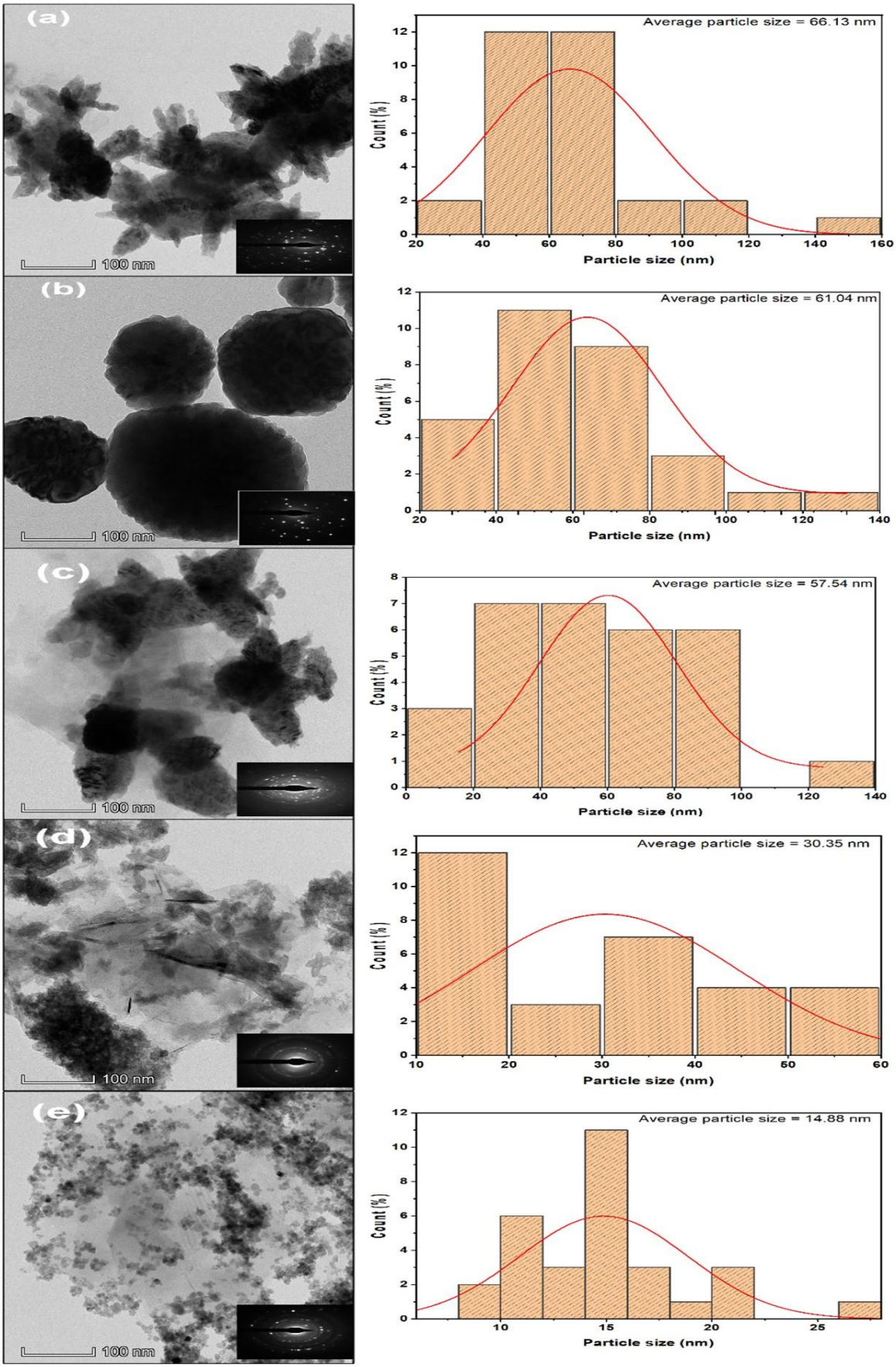

Figure 5. Image of TEM, the histogram for particle size distribution and SAED pattern of (a) ZnO, (b) Fe_2O_3, (c) ZnO/rGO, (d) Fe_2O_3/rGO and (e) $ZnOFe_2O_3$/rGO.

The FESEM image in Figure 4c demonstrates the attachment of ZnO composite anchoring onto rGO by cooperating with the remaining functional groups of rGO. Due to that, the average diameter size of ZnO in the composite is relatively smaller than that of pure ZnO material. Figure 4b displays spherical-like particles of Fe_2O_3 with uniform size. Figure 4d portrays the even scattering of Fe_2O_3 nanoparticles on the wrinkled surface of rGO sheets. The high surface area was achieved by encapsulating Fe_2O_3 nanoparticles within the rGO sheets, which prevents the accumulation of rGO sheets and aggregation of individual nanoparticles [13]. ZnO and Fe_2O_3 characteristics are evident in the flake-like morphology of the ternary composite (Figure 4e), which grew over folded sheets of rGO.

Consequently, TEM analyzed the size and shapes of the synthesized samples at various magnifications. From Figure 5, uniform sizes and distribution were achieved through hydrothermal synthesis. The effect of adding rGO to the composites results in multiple shapes and darker spots, which are distributed over the surface of the ZnO and Fe_2O_3 shown in Figures 5c, d, and e. Interestingly, the mean particle size of the binary and ternary composite was smaller with the addition of graphene compared to the single metal oxide. The 2D structure of the graphene allows efficient nucleation and growth of the nanoparticles by providing a large surface area for the nanoparticles, leading to smaller particle sizes. Aside from that, the interaction between the ZnO, Fe_2O_3 and rGO influences the particle size of the composite by preventing the agglomeration of the nanoparticles [14-15]. According to the histogram bar in the inset of Figure 5, the mean particle sizes of ZnO, Fe_2O_3, ZnO/rGO, Fe_2O_3/rGO and $ZnOFe_2O_3$/rGO are $\pm$ 66.13 nm, $\pm$ 61.04 nm, $\pm$ 57.52 nm, $\pm$ 30.35 nm and $\pm$ 14.88 nm, respectively. The Selected Area Electron Diffraction (SAED) pattern, depicted in the inset of Figure 5, was utilized to investigate the crystalline nature of the prepared composite. Correspondingly, the bright pattern rings confirmed the polycrystallinity of the synthesized materials corresponding to the XRD analysis. Overall, adding graphene to the composite resolves the agglomeration, resulting in reduced particle sizes but an increased surface-to-volume ratio for efficient electrochemical sensing performances.

Electrochemical Measurement

The characteristics of electrochemical performance for the modified electrodes were measured by CV analysis. The measurement was taken in the presence and absence of 5 mM glucose by applying the potential at 0.0 to 1.0, and the scan rate was set to 50 mV s^{-1}, as shown in Figure 6. From Figure 6a, ZnO/rGO, Fe_2O_3/rGO, and $ZnOFe_2O_3$/rGO electrodes display significant responses compared to ZnO and Fe_2O_3 electrodes. Moreover, no prominent peak of oxidation is observed at ZnO and Fe_2O_3 electrodes compared to ZnO/rGO, Fe_2O_3/rGO, and $ZnOFe_2O_3$/rGO electrodes. On the other hand, wider curves and higher current density were observed in the presence of glucose, as shown in Figure 6b. The current density measured for the modified electrodes is listed in Table 1.

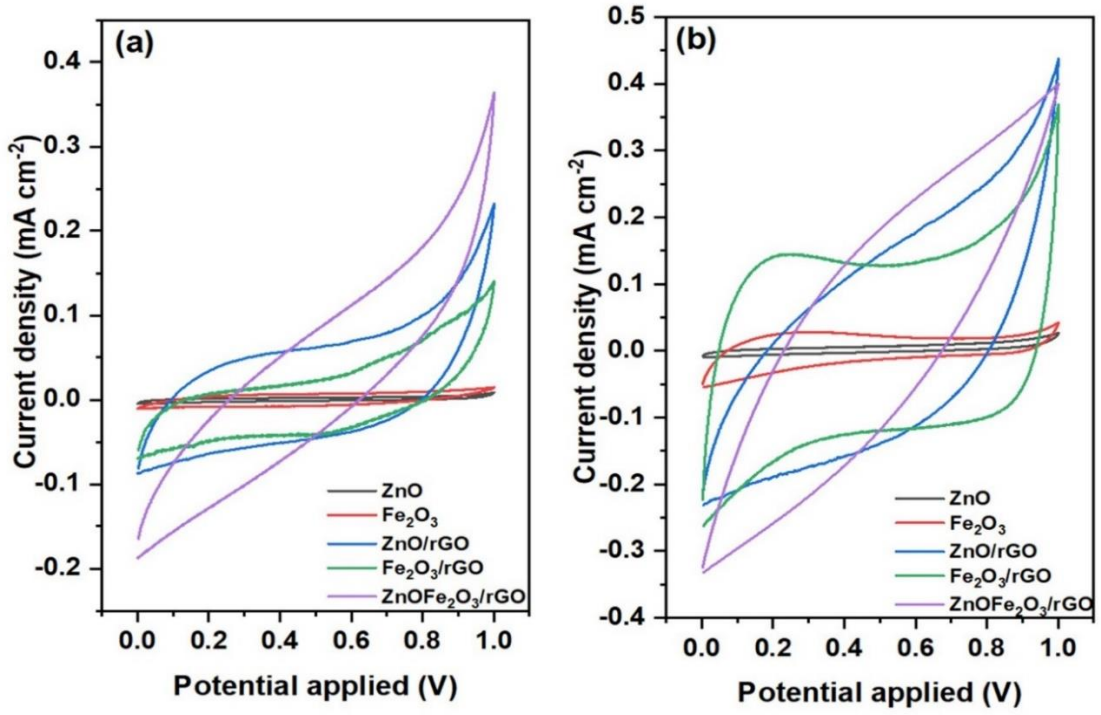

Figure 6. CV response of ZnO Fe_2O_3, ZnO/rGO, Fe_2O_3/rGO, and ZnO Fe_2O_3/rGO in a) 0.1 M PBS b) 0.1 M PBS with 5 mM glucose.

Table 1. The current measurement of the modified electrode is in the absence and presence of glucose.

Electrode	Current density (mA cm^{-2})	
	0.1M PBS	**0.1 M PBS + 5 mM Glucose**
ZnO	0.0011	0.0032
Fe_2O_3	0.0055	0.0276
ZnO/rGO	0.0459	0.1928
Fe_2O_3/rGO	0.0220	0.1372
$ZnOFe_2O_3$/rGO	0.0775	0.2099

Table 1 demonstrates that the anodic peak current of $ZnOFe_2O_3$/rGO was approximately 66 times and 8 times greater than the ZnO nanoparticle and Fe_2O_3 nanoparticle, respectively, in the potential window of 0.56 V. The enhanced electrochemical performance is due to the expanded area of the surface resulting from the decreased size of particles induced by the collaborative effects of the ZnO, Fe_2O_3 and rGO components in the compound system [14]. The conductivity of the composite was enhanced with the addition of rGO in the system and contributed to the nanocomposite's large surface area, allowing more contact with glucose [14].

The CV response of the modified electrodes on different glucose concentrations is conducted to verify the impact of glucose on the resultant currents, as shown in Figure 7a. Based on the observed increase in peak current, it can be deduced that modified electrodes fit the glucose electrocatalytic oxidation, particularly in the presence of high glucose concentrations [16]. To ascertain the sensitivity and Limit of Detection (LOD), the linear plot of the prepared electrode was plotted between the current of catalytic oxidation and the glucose concentration, as shown in Figure 7b. The glucose concentration varies from 1, 2, 5,7 and 10 mM. Sensitivity is a statistical indicator that reflects the performance of a sensor; the slope of the plotted linear graph indicates the electrode's sensitivity. The linear regression equation is derived as Jpeak = 0.0358C, where Jpeak represents the current density, and C is the glucose concentration with a correlation coefficient (R^2) of 0.9682 [16-17]. Subsequently, the slope of function was utilized to compute the sensitivity and LOD, which were determined to be 504.23 µA mM^{-1} cm^{-2} and 6.28 mM, respectively.

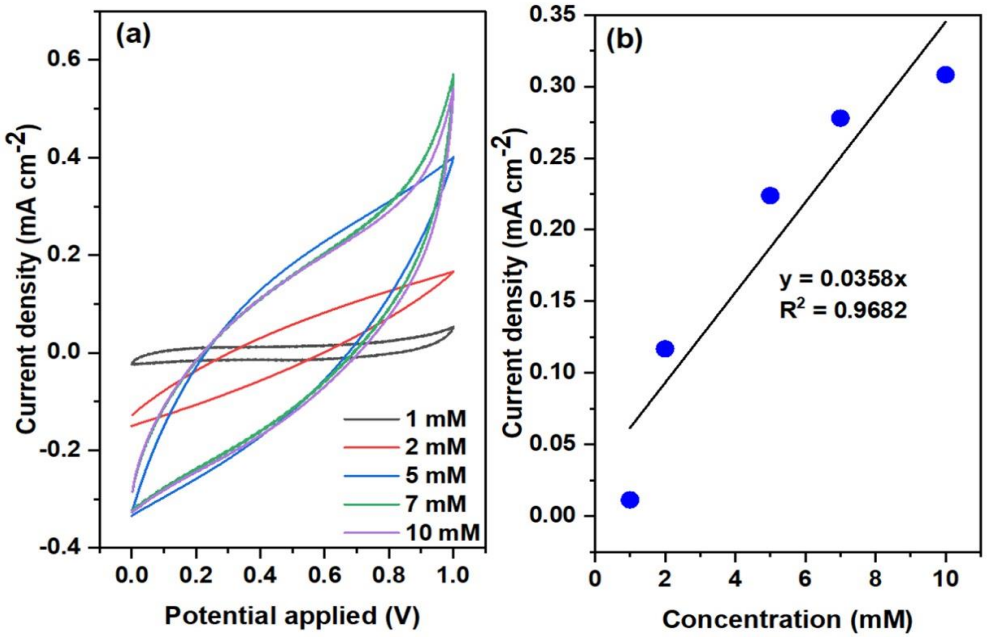

Figure 7 (a) CV response of the $ZnOFe_2O_3$/rGO electrode at diverse glucose concentrations and (b) linear plot for peak current against the square root of scan rate for the $ZnOFe_2O_3$/rGO electrode.

Table 2. Comparison of the $ZnOFe_2O_3$/rGO modified electrode with other ZnO and Fe_2O_3-based glucose sensors.

Electrode Material	Method of Synthesis	Sensitivity, $\mu A.\, mM^{-1}.\, cm^{-2}$	Detection limit, µM	Reference
ZnO-CoO/rGO	Hydrothermal	168.7	1.3	[1]
ZnO-Ag/rGO	Microwave-assisted	-	10.6	[19]
ZnO@rGO	Microwave-assisted	481	0.008	[20]
ZnO-Cu	Sol-gel	-	0.01	[21]
GF/ Fe_2O_3	Hydrothermal	20.03	71.6	[22]
Fe_2O_3 nanowires	Wet chemical method	726.9	-	[23]
Fe_2O_3-Ag/rGO	Hydrothermal	50.8	0.5	[24]
$Fe_2O_3/ZnFe_2O_4$	Combustion	609	-	[18]
$ZnOFe_2O_3$/rGO	Hydrothermal	504.32	6.28 mM	Present work

The improved surface area distribution of $ZnOFe_2O_3$ nanocomposite on the graphene oxide increased the active adsorption sites, making them responsible for the exceptional sensitivity and wide linear range observed in glucose detection [18]. The results obtained are compared with those of the previously reported glucose biosensors based on ZnO or Fe_2O_3 nanomaterials in Table 2. Thus, it is worth mentioning that the $ZnOFe_2O_3$/rGO electrode can be modified into an electrochemical glucose sensor with a sensitivity of 504.32 µA mM^{-1} cm^{-2}, as indicated by the electrochemical studies.

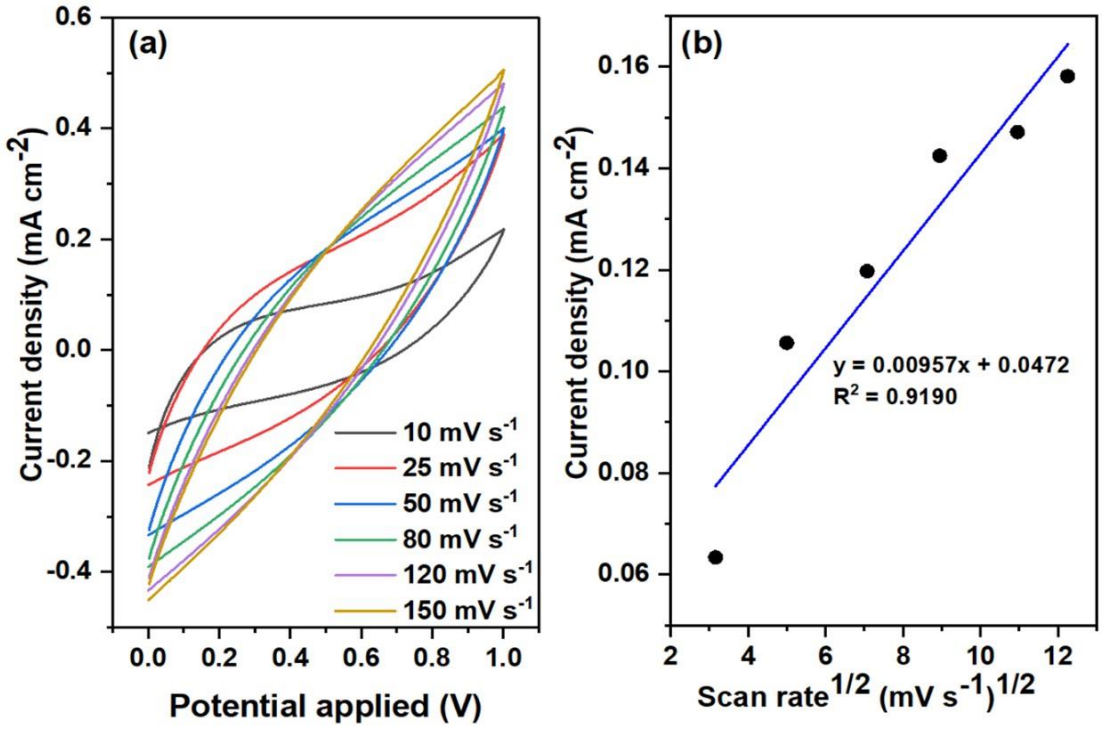

Figure 8. (a) CV response of $ZnOFe_2O_3$/rGO electrode at scan rates of 10-150 mV s^{-1} and (b) linear plot peak current against the square root of scan rate for $ZnOFe_2O_3$/rGO electrode.

Additionally, the electron transfer mechanism of the prepared electrodes was determined through CV analysis in the identical medium at diverse scan rates varying from 10 to 150 mV s^{-1}. The anodic current (I_{pa}) for the ZnO, Fe_2O_3, ZnO/rGO, Fe_2O_3/rGO and $ZnOFe_2O_3$/rGO increased linearly with the increased scan rate. Anodic and cathodic peaks also show noticeable shifts towards negative and positive directions, as in Figure 8. A linear trend with a correlation coefficient of 0.9190 is observed when the anode peak currents of the ZnO Fe_2O_3/rGO in 0.1M PBS with 5 mM glucose are plotted against the square root of the scan rate (Figure 8b). This indicates that the electrocatalysis of glucose involves a process that is controlled by diffusion [16, 17, 25].

CONCLUSION

FESEM and TEM analysis revealed flower-like ZnO and spherical Fe_2O_3 particles. In addition, introducing rGO into the composite presents well-dispersed ZnO and Fe_2O_3 nanoparticles on the wrinkled sheet surface of rGO. The electrochemical sensing revealed that the $ZnOFe_2O_3$/rGO electrode has strong sensitivity towards glucose, with a value of 504.32 $\mu A.mM^{-1}.cm^{-2}$ and glucose detection limit of 6.28 mM, attributed to superior conductivity and rapid electron transfer stability of ZnO, exceptional stability of Fe_2O_3, and graphene's high surface area and conductivity. Based on excellent performance, we believe $ZnOFe_2O_3$/rGO can be adapted as the nonenzymatic glucose sensor for clinical diagnosis and food processing quality control.

ACKNOWLEDGEMENTS

Authors acknowledge the Ministry of Higher Education (MOHE) for funding under the Fundamental Research Grant Scheme (FRGS) (FRGS/1/2021/TK0/UNIKL/ 02/8).

REFERENCES

1. Wang, M., Ma, J., Chang, Q., Fan, X., Zhang, G., Zhang, F., Peng, W. and Li, Y. (2018) Fabrication of a novel ZnO–CoO/rGO nanocomposite for nonenzymatic detection of glucose and hydrogen peroxide. *Ceramics International*, **44(5)**, 5250–5256.

2. World Health Organization (2021) *Global Report on Diabetes* https://www.who.int/news-room/fact-sheets/detail/diabetes.

3. Hassan, M. H., Vyas, C., Grieve, B. and Bartolo, P. (2021) Recent Advances in Enzymatic and Nonenzymatic Electrochemical Glucose Sensing. *Sensors*, **21(4672)**.

4. Faridbod, F., Gupta, V. K. and Zamani, H. A. (2011) Electrochemical Sensors and Biosensors. *International Journal of Electrochemistry*, 1-2.

5. da Trindade, L. G., Hata, G. Y., Souza, J. C., Soares, M. R. S., Leite, E. R., Pereira, E. C., Longo, E. and Mazzo, T. M. (2020) Preparation and characterization of hematite nanoparticles-decorated zinc oxide particles (ZnO/Fe_2O_3) as photoelectrodes for solar cell applications. *Journals of Material Science*, **55(7)**, 2923–2936.

6. Hwa, K. Y., Santhan, A. and Tata, S. K. S. (2020) Fabrication of Sn-doped ZnO hexagonal micro discs anchored on rGO for electrochemical detection of anti-androgen drug flutamide in water and biological samples. *Microchemical Journal*, **160**, 105689.

7. Parihar, V., Raja, M. and Paulose, R. (2018) A brief review of structural, electrical and electrochemical properties of zinc oxide nanoparticles. *Reviews on Advanced Materials Science*, **53(2)**, 119–130.

8. Liu, L., Zhao, C., Zhao, H., Zhang, Q. and Li, Y. (2014) ZnO-CoO nanoparticles encapsulated in 3D porous carbon microspheres for high-performance lithium-ion battery anodes. *Electrochimica Acta*, **135**, 224–231.

9. Hwa, K. Y., Sharma, T. S. K. and Ganguly, A. (2020) Design strategy of rGO-HNT-AgNPs based hybrid nanocomposite with enhanced performance for electrochemical detection of 4-nitrophenol. *Inorganic Chemistry Front*, **7(10)**, 1981–1994.

10. Yang, S., Li, M., Guo, Z., Xia, N. and Qu, L. (2019) Facile Synthesis of Fe-MOF/rGO nanocomposite as an Efficient Electrocatalyst for Nonenzymatic H_2O_2 Sensing. *International Journal of Electrochemical Science*, **14**, 7703–7716.

11. Alver Tascıoğlu, M. E., Güler, O., Aslan, M., Yazgan, A., Kaya, H., Duran, C., Çuvalcı, H. and Bilgin, S. (2019) Optical and Dielectric Properties of PMMA/α-Fe_2O_3–ZnO Nanocomposite Films. *Journal of Inorganic and Organometallic Polymers and Materials*, **29(5)**, 1514–1522.

12. Banerjee, S., Naha, S. and Puri, I. K. (2008) Molecular simulation of the carbon nanotube growth mode during catalytic synthesis. *Applied Physics Letters*, **92(23)**, 2006–2009.

13. Bharath, G., Anwer, S., Mangalaraja, R. V., Alhseinat, E., Banat, F. and Ponpandian, N. (2018) Sunlight-Induced photochemical synthesis of Au nanodots on α-Fe_2O_3@Reduced graphene oxide nanocomposite and their enhanced heterogeneous catalytic properties. *Scientific Reports*, **8(1)**, 1–14.

14. Hussein, B. A., Tsegaye, A. A., Shifera, G. and Taddesse, A. M. (2023) A sensitive nonenzymatic electrochemical glucose sensor based on a ZnO/

Co_3O_4/reduced graphene oxide nanocomposite. *Sensors and Diagnostics*, **2(2)**, 347–360.

15. Rasuli, H. and Rasuli, R. (2023) Nanoparticle-decorated graphene/graphene oxide: synthesis, properties and applications. *Journals of Material Science*, **58**, 2971–2992.

16. Gopal, T. S., Jeong, S. K., Alrebdi, T. A., Pandiaraj, S., Alodhayb, A., Muthuramamoorthy, M. and Andrews, N. G. (2022) MXene-based composite electrodes for efficient electrochemical sensing of glucose by nonenzymatic method. *Materials Today Chemistry*, **24**.

17. Abrori, S. A., Luh, N., Septiani, W., Anshori, I., Suendo, V. and Yuliarto, B. (2020) Nonenzymatic Electrochemical Detection of Glucose. *Sensors*, **20**, 4891–4907.

18. Neravathu, D., Paloly, A. R., P. S. M. S. and Bushiri, M. J. (2020) Hybrid nanomaterial of $ZnFe_2O_4$/α-Fe_2O_3 implanted graphene for electrochemical glucose sensing application. *Diamond and Related Materials*, **106(March)**, 107852.

19. Li, Z., Sheng, L., Meng, A., Xie, C. and Zhao, K. (2016) A glassy carbon electrode modified with a composite consisting of reduced graphene oxide, zinc oxide and silver nanoparticles in a chitosan matrix for studying the direct electron transfer of glucose oxidase and for enzymatic sensing of glucose. *Microchimica Acta*, **183(5)**, 1625–1632.

20. Babitha, K. B., Soorya, P. S., Peer Mohamed, A., Rakhi, R. B. and Ananthakumar, S. (2020) Development of ZnO@rGO nanocomposites for the enzyme free electrochemical detection of urea and glucose. *Materials Advances*, **1(6)**, 1939–1951.

21. Mahmoud, A., Echabaane, M., Omri, K., Boudon, J., Saviot, L., Millot, N. and Chaabane, R. B. (2021) Cu-doped ZnO nanoparticles for nonenzymatic glucose sensing. *Molecules*, **26(4)**.

22. Güneş, F., Aykaç, A., Erol, M., Erdem, Ç., Hano, H., Uzunbayir, B., Şen, M. and Erdem, A. (2022) Synthesis of hierarchical hetero-composite of graphene foam/α-Fe_2O_3 nanowires and its applications on glucose biosensors. *Journals of Alloys Compounds*, **895(2)**.

23. Cao, X. and Wang, N. (2011) A novel nonenzymatic glucose sensor modified with Fe_2O_3 nanowire arrays. *Analyst*, **136(20)**, 4241–4246.

24. Zhang, N. and Zheng, J. (2017) Synthesis of Ag–Fe_2O_3–RGO nanocomposites for the electrocatalytic reduction of H_2O_2. *Journals of Materials Science: Materials in Electronics*, **28(15)**, 11209–11216.

25. Wang, L., Han, M., Shuck, C. E., Wang, X. and Gogotsi, Y. (2021) Adjustable electrochemical properties of solid-solution MXenes. *Nano Energy*, **88(July)**, 1–8.